IEEE Access
Multidisciplinary | Rapid Review | Open Access Journal

Received December 24, 2017, accepted January 18, 2018, date of publication January 23, 2018,
date of current version February 28, 2018.

Digital Object Identifier 10.1109/ACCESS.2018.2797216

An Improved Ambiguity Resolution of Three Carriers in Precise Point Positioning

XIAOYING GU AND BOCHENG ZHU
School of Electronics Engineering and Computer Science, Peking University, Beijing 100871, China

Corresponding author: Xiaoying Gu (guxiaoying@pku.edu.cn)

This work was supported by the State Administration of Science, Technology and Industry for National Defense under Grant JCKY2016110B004.

ABSTRACT Precise point positioning (PPP) is of great importance in fields requiring coordinates with high accuracy, such as geophysics, meteorology, and geodesy. Compared with relative positioning restricted by the length of baseline, PPP using a single receiver is more flexible. Carrier phase observations with much higher precision than pseudorange measurements are used in the positioning process of PPP. However, accurate estimation of integer ambiguity associated with carrier phase observations is a prerequisite. Then the integrity of the phase observable can be completed as a range measurement with high precision. With triple-frequency signals of global navigation satellite system (GNSS) available, combinations of original observations with longer wavelengths and lower noises are preferable. In this paper, we propose an improved ambiguity resolution (AR) method based on the traditional bootstrapping method to make it suitable for PPP and increase the precision of AR and positioning. Virtual ambiguities of extra-wide-lane, wide-lane, and modified narrow-lane combinations are resolved first for their relatively better characteristics. Furthermore, extra pseudoranges are included to decrease the ionospheric delay which cannot be ignored as it is in relative positioning. Then, original ambiguities on the three frequencies can be recovered from the combined ambiguities using three linear equations which are independent to each other. Finally, the performance of the improved method is tested with real GPS navigation data on three frequencies which is provided by the international GNSS service. Compared with the traditional bootstrapping method, it shows that the ambiguity residuals of the improved method have decreased which indicates more accurate estimation. The precision of the positioning results has increased accordingly.

INDEX TERMS GNSS, GPS, ambiguity resolution, precise point positioning, triple-frequency positioning.

I. INTRODUCTION

Precise point positioning is widely used in fields such as high precision navigation, geophysics, meteorology, geodetic and so on. In relative positioning, the length of the baseline between the user and the reference receivers usually restrict the application and precision of this method severely. The double-differenced biases such as orbital, ionospheric and tropospheric residuals will increase with the increment of distance between the user and the reference receivers. The errors of the medium and long baselines can't be eliminated effectively as the ones of the short baselines ($< 10km$) [1]. However, depending on a single receiver, PPP is more flexible and won't be affected by length of the baseline. In recent years, the satellite orbit and clock products provided by several institutions such as IGS are becoming more accurate and timely. What's more, the strategies of network analysis to derive integrated estimation of the station coordinates and satellite orbits as well as Earth rotation parameters with full statistical information are steadily improved. Therefore positioning results with decimeter or even centimeter accuracy in PPP are possible [2]–[4]. Soycan and Ata [5] (2011) investigated the availability of precise point positioning and compared it to the traditional network solution. They concluded that PPP may be an alternative to traditional relative positioning. Thus PPP using a single receiver is considered to be a powerful tool that can be applied to the fields such as crustal deformation monitoring, near real-time GPS meteorology, orbit determination of low Earth orbiting satellites, and the precise positioning of mobile objects. In conclusion PPP is becoming a very pragmatic tool.

Pseudorange measurement which is primarily used for navigation nowadays has measuring error of meter-scale.

Hence it is not qualified for high precision positioning. In PPP, carrier phase observations are utilized because they have much lower measurement noises than the code observations. As it is known, the cycles of the carrier phase observations are counted after acquisition of the satellite signal by the receiver. As a result, the integer cycles before acquisition are not known in advance and are named as integer ambiguities. With the integrated measurement unknown, the carrier phase observables can't be applied to the positioning process straightly. Hence, accurate estimation of the integer ambiguity associated with the carrier phase is a prerequisite for high precision positioning. Once the integer ambiguity has been resolved, carrier phase measurement can be used as the parameter of range as the pseudorange does however with much higher positioning accuracy.

In order to improve the positioning precision of PPP, many approaches related to ambiguity resolution have been put forward in recent years. Normally in preprocessing, the ambiguity won't keep the integer property naturally due to the existence of uncalibrated errors originated in the receiver and satellite [6]–[8]. In summary, precise modeling or thorough elimination of the error sources which bias the code and carrier phase observations are vital for reliable ambiguity resolution in any system of GNSS [9]. In one hand, fractional-cycle biases (FCBs) in the float estimations were proposed to be eliminated by Geng *et al.* [10] (2010). Geng *et al.* [11] (2010) theoretically proved the equivalence of the ambiguity-fixed position estimates derived from two different methods by assuming that the FCBs were hardware-dependent and they were only assimilated into the clocks and ambiguities. On the other hand, new strategies were presented to remove the uncalibrated phase delays (UPDs). XX Li (2013) developed a real-time computational procedure for generating uncalibrated phase delays (UPDs) on L_1 and L_2 frequencies. The empirical spatial and temporal constraints and the ionospheric delays derived from a real-time available ionospheric model were all considered as pseudo-observations into the estimation for strengthening the solution [12]. Ge *et al.* [13] (2008) demonstrated that the single-differenced (SD) UPDs between satellites in wide-lane and narrow-lane combinations from a global reference network could be estimated with high accuracy through a statistical analysis of the ambiguities. Thus the corrected SD-ambiguities could be fixed to integer values.

Apart from the operation of single difference, AR for zero-differenced (ZD) PPP had been put forward. Zhang *et al.* [14] (2013) investigated and demonstrated the performance of a global zero-differenced (ZD) PPP integer ambiguity resolution (IAR) service for GPS users by providing routine ZD uncalibrated fractional offsets (UFOs) for wide-lane and narrow-lane combinations. In the work of Zhang *et al.* [15] (2011), the ZD GNSS observations from a regional reference network were processed based upon re-parameterized observation equations, corrections for satellite clocks, phase biases and interpolated atmospheric delays were calculated and provided to users. In the second step, these network-based corrections were used at the user site to restore the integer nature of the ZD phase ambiguities, which made rapid and high accuracy user positioning possible. What's more, the corrections from the networks were utilized for single point positioning. Bertiger *et al.* [16] (2010) presented an algorithm processing dual-frequency GPS data from a single receiver together with wide-lane and phase bias estimates from the global network of GPS receivers. The algorithm was demonstrated to have significantly improved repeatability of daily estimates of ground receiver position. Le *et al.* [17] (2009) investigated the use of Global and Regional Ionosphere Maps for single-frequency precise point positioning. The results showed that the SWACI map could bring the vertical positioning accuracy to the same level as the horizontal one, at 23 km. Teunissen *et al.* [18] (2010) discussed the concept of PPP-RTK. By forming certain combinations of these network parameters for correcting their single-receiver GNSS phase and code data, users could perform integer ambiguity resolution and realize cm-level positioning.

As we can see, the precision of the float ambiguity resolution is the foundation of the following fixation procedures for almost all methods. So it is vital to improve the precision of the float ambiguity resolution either. Then the parameters of interest (e.g. receiver coordinates) can be calculated with a higher precision. With triple-frequency signals of GNSS available, the virtual signals with longer wavelengths and lower noises can be constructed through linear combinations. Therefore, we propose an improved ambiguity resolution method for PPP based on the triple-frequency carriers and the traditional boot-strapping method in order to increase the precision of the AR and the positioning. Considering the characteristics of different combinations along with the success rates, the relatively better virtual signals named as extra-wide-lane, wide-lane and modified narrow-lane combinations are chosen for AR. In the traditional methods designed for relative positioning, the ionospheric residuals after double difference are small enough to be neglected. In order to eliminate the geometry parameters and residual ionospheric delays of single receiver, extra pseudoranges are combined with the optimal combinations to reduce the ionospheric errors in the improved method. With real GPS navigation data on three frequencies, the effectiveness of the improved method is tested by numerical analysis. The ambiguity fixing results and the positioning precision of the improved method are compared with that of the traditional boot-strapping method.

The paper is organized as follows. In section 2, we first introduce the mathematical models and the resolution of the observation equations of the positioning process using the triple-frequency code and carrier phase measurements in PPP. Then in the next section, we interpret the basic procedures of boot-strapping methods using combinations of triple-frequency observables. In section 4, the procedures of the improved method which is suitable for PPP and will achieve more reliable ambiguity resolution are presented. Section 5 illustrates the results and analysis of the numeri-

cal test using the improved method and traditional method respectively. Conclusion comes as the last section.

II. OBSERVATION EQUATIONS OF CODE AND CARRIER PHASE

The code (P or C/A) and carrier phase observations included in the GNSS signals are used for positioning and ambiguity resolution of PPP. Although the functions of the observables have been discussed sufficiently before, they still need to be introduced first as foundations of positioning. The mathematical equations of the original code and carrier phase observations on multiple frequencies are expressed as [19]:

$$P_i = \rho + \beta_{1i}\delta I_1 + \varepsilon_{P_i} \tag{1}$$

$$\Phi_i = \rho - \beta_{1i}\delta I_1 - \lambda_i N_i + \varepsilon_{\Phi_i} \tag{2}$$

where the subscript i denotes various frequencies of GNSS. P_i and Φ_i indicate the code and phase observables in meters; ρ is the geometric parameter which doesn't change with the variances of the frequencies and includes the distances between receivers and satellites, the receiver and satellite hardware delays in meters and clock errors, along with the tropospheric delays. The symbol δI_1 denotes the ionospheric bias on frequency f_1 in meters, $\beta_{1i} = f_1^2/f_i^2$ is the ionospheric scale factor (ISF), λ_i is the wavelength of f_i, N_i is the integer ambiguity in cycles. ε_{P_i} and ε_{Φ_i} are the code and phase measurement noises including multipath noise on frequency f_i and they are independent to each other.

In PPP, most of the main errors are corrected in the preprocessing procedure. For example, the satellite clock errors can be corrected by interpolation of the precise ephemeris provided by analysis system such as IGS [20]. The dry component of the tropospheric delays can be computed approximately by interpolation of the Saastamoinen model or the UNB3 model [21]. Hence the coordinates, the residual wet component of the tropospheric delays, ionosphere delays and the integer ambiguities are the mainly remaining unknown parameters.

For these non-linear observation equations, generally the least-square (LS) method is used to resolve the unknown parameters of interest. Supposed that the ambiguity parameter N_i has been resolved precisely, then the coordinates of the receiver can be resolved by the equations written as:

$$\begin{bmatrix} \boldsymbol{P} \\ \boldsymbol{\Phi} + \boldsymbol{\lambda N} \end{bmatrix} = \boldsymbol{GX} + \begin{bmatrix} \boldsymbol{\varepsilon_P} \\ \boldsymbol{\varepsilon_\Phi} \end{bmatrix} \tag{3}$$

where $\boldsymbol{G}$ is the geometric matrix of the LS method. Hence, if we can improve the precision of the float ambiguity estimation so that it can be fixed to a more precise integer ambiguity correspondingly, more accurate positioning results can be derived.

Up to now many methods to resolve the ambiguity have been proposed. Teunissen *et al.* [22] made a comparison between the LAMBDA method and boot-strapping methods such as the Three-Carrier Ambiguity Resolution (TCAR) and the Cascading Integer Resolution (CIR) method [23], [24]. The LAMBDA method utilizes the information of variance-covariance matrix and the statistical decorrelation for ambiguity transformation to search for the integer ambiguity. The boot-strapping method is generally based on a group of selected linear combinations of the original multi-frequency observations. Although the LAMBDA method will achieve relatively higher success rate, it will involve much more complexity of computation due to decorrelation and the procedure of integer searching. On the contrary, with linear combinations, the computations of the boot-strapping methods are much easier. On the other hand, with signals on more frequencies accessible to users nowadays, boot-strapping methods utilizing multiple frequencies will get novel benefits for AR. Hence, the procedures to improve the resolution accuracy of boot-strapping method is of interest and introduced in the following sections.

III. LINEAR COMBINATIONS OF OBSERVATIONS

As it is known, some systems of the GNSS such as the modern GPS (Global Positioning System) and BDS (Beidou Navigation Satellite System) have been broadcasting signals on three frequencies. With code and carrier phase observations on more and more frequencies available, more combinations of triple-frequencies utilized for boot-strapping method can be constructed. Hence, new combinations characterized to have longer wavelengths and lower measurement noises than the preceding ones of single or double frequencies are more likely to be obtained. These characters will contribute to increase the accuracy and efficiency of integer ambiguity resolution and positioning. As basic knowledge of the improved method in the next section, the traditional boot-strapping method is elaborated first [25]. The mathematical model commonly used in this kind of method is introduced in the following part.

A. LINEAR COMBINATION OF THE CODE AND CARRIER PHASE OBSERVATIONS

In order to deduce the corresponding virtual parameters of the combined equations, both sides of equation (2) are divided by the wavelength and the derivation is expressed as:

$$L_i = \lambda_i^{-1}(\rho - \beta_{1i}\delta I_1) - N_i + \varepsilon_{\Phi_i} \tag{4}$$

where $L_i = \Phi_i\lambda^{-1}$ represents the observable of the carrier phase in the unit of cycles. The definitions of the symbols ρ, β_{1i}, δI_1 and N_i are the same as they are in the original measurement models (2). For satellite signals with three frequencies, the subscript i is assigned as 1, 2 or 3. Then the corresponding carrier phases on the three frequencies can be written as L_1, L_2 and L_3. They are arranged according to the magnitude of the three wavelengths λ_1, λ_2, and λ_3, which satisfy the relationship of $\lambda_1 < \lambda_2 < \lambda_3$. Then arbitrary coefficients written as k_1, k_2 and k_3 are assumed to be the combination parameters of L_1, L_2 and L_3. Hence the equation linearly combined by the original triple-frequency

observations is written as:

$$\begin{aligned} L_{(k_1,k_2,k_3)} &= k_1L_1 + k_2L_2 + k_3L_3 \\ &= (\frac{k_1}{\lambda_1} + \frac{k_2}{\lambda_2} + \frac{k_3}{\lambda_3})\rho - (\frac{k_1}{\lambda_1} + \frac{k_2\lambda_2}{\lambda_1^2} + \frac{k_3\lambda_3}{\lambda_1^2})\delta I_1 \\ &\quad - N_{(k_1,k_2,k_3)} + \varepsilon_{\Phi_{(k_1,k_2,k_3)}} \end{aligned} \tag{5}$$

where $N_{(k_1,k_2,k_3)}$ represents the combined ambiguity of the virtual carrier phase and is derived as:

$$N_{(k_1,k_2,k_3)} = k_1 \cdot N_1 + k_2 \cdot N_2 + k_3 \cdot N_3 \tag{6}$$

To preserve the integer character of the combined ambiguity $N_{(k_1,k_2,k_3)}$, the combination parameters k_1, k_2 and k_3 are required to be integers as well, in order that $N_{(k_1,k_2,k_3)}$ can be resolved in the same way as the original integer ambiguity. Consequently, when equations (1) and (2) are combined by the coefficients of k_1, k_2, and k_3, the combined code and carrier phase observations are derived as:

$$\begin{aligned} P_{(k_1,k_2,k_3)} &= \frac{k_1 \cdot f_1 \cdot P_1 + k_2 \cdot f_2 \cdot P_2 + k_3 \cdot f_3 \cdot P_3}{k_1 \cdot f_1 + k_2 \cdot f_2 + k_3 \cdot f_3} \\ &= \rho + \beta_{(k_1,k_2,k_3)}\delta I_1 + \varepsilon_{P_{(k_1,k_2,k_3)}} \end{aligned} \tag{7}$$

$$\begin{aligned} \Phi_{(k_1,k_2,k_3)} &= \frac{k_1 \cdot f_1 \cdot \Phi_1 + k_2 \cdot f_2 \cdot \Phi_2 + k_3 \cdot f_3 \cdot \Phi_3}{k_1 \cdot f_1 + k_2 \cdot f_2 + k_3 \cdot f_3} \\ &= \rho - \beta_{(k_1,k_2,k_3)}\delta I_1 - \lambda_{(k_1,k_2,k_3)}N_{(k_1,k_2,k_3)} \\ &\quad + \varepsilon_{\Phi_{(k_1,k_2,k_3)}} \end{aligned} \tag{8}$$

where $\beta_{(k_1,k_2,k_3)}$ is the ionospheric scalar factor of the combined signal with reference to the one of carrier L_1. The combined ISF is expressed as:

$$\beta_{(k_1,k_2,k_3)} = \frac{f_1^2 \cdot (k_1/f_1 + k_2/f_2 + k_3/f_3)}{k_1 \cdot f_1 + k_2 \cdot f_2 + k_3 \cdot f_3} \tag{9}$$

According to the procedure of the derivation, the virtual frequency and wavelength of the linearly combined observation are expressed as:

$$f_{(k_1,k_2,k_3)} = k_1 \cdot f_1 + k_2 \cdot f_2 + k_3 \cdot f_3 \tag{10}$$

$$\lambda_{(k_1,k_2,k_3)} = \frac{c}{k_1 \cdot f_1 + k_2 \cdot f_2 + k_3 \cdot f_3} \tag{11}$$

where c represents the speed of light in vacuum. Under common situations, the noises of the pseudorange measurements on different frequencies are assumed to be identical and independent to each other, which are expressed as $\sigma_{P_1} = \sigma_{P_2} = \sigma_{P_3} = \sigma_P$ with decimeter level. Similarly, for the carrier phase noises which are also independent and identical to each other, the standard variances meet the equation of $\sigma_{\Phi_1} = \sigma_{\Phi_2} = \sigma_{\Phi_3} = \sigma_\Phi$ with millimeter level. Without loss of generality, it can be assumed that $\sigma_P = 0.25$ m and $\sigma_\Phi = 0.002$ m for common circumstance [26]. Therefore, the variances of code and carrier phase observations after linear combination are derived as:

$$\begin{aligned} \sigma^2_{P_{(k_1,k_2,k_3)}} &= \frac{(k_1 \cdot f_1)^2 \cdot \sigma^2_{P_1} + (k_2 \cdot f_2)^2 \cdot \sigma^2_{P_2} + (k_3 \cdot f_3)^2 \cdot \sigma^2_{P_3}}{(k_1 \cdot f_1 + k_2 \cdot f_2 + k_3 \cdot f_3)^2} \\ &= \eta^2_{(k_1,k_2,k_3)}\sigma_P^2 \end{aligned} \tag{12}$$

$$\begin{aligned} \sigma^2_{\Phi_{(k_1,k_2,k_3)}} &= \frac{(k_1 \cdot f_1)^2 \cdot \sigma^2_{\Phi_1} + (k_2 \cdot f_2)^2 \cdot \sigma^2_{\Phi_2} + (k_3 \cdot f_3)^2 \cdot \sigma^2_{\Phi_3}}{(k_1 \cdot f_1 + k_2 \cdot f_2 + k_3 \cdot f_3)^2} \\ &= \eta^2_{(k_1,k_2,k_3)}\sigma_\Phi^2 \end{aligned} \tag{13}$$

where $\eta_{(k_1,k_2,k_3)}$ represents the phase noise factor (PNF) and is derived as:

$$\eta^2_{(k_1,k_2,k_3)} = \frac{(k_1 \cdot f_1)^2 + (k_2 \cdot f_2)^2 + (k_3 \cdot f_3)^2}{(k_1 \cdot f_1 + k_2 \cdot f_2 + k_3 \cdot f_3)^2} \tag{14}$$

B. PROCEDURES OF BOOT-STRAPPING METHODS

For boot-strapping methods, the virtual ambiguities are usually resolved from the combinations with longer wavelengths to the ones with shorter wavelengths sequentially. However, most of the linear combinations are not qualified to be used for the ambiguity resolution because of the short wavelength, large ionospheric delay or high combination noise. So how to choose the optimal set of the combinations is vital to the boot-strapping method.

As for the boot-strapping method, it starts with the extra-wide-lane (EWL) combination of the two closest L-band carriers. Then the float ambiguity of EWL combination can be resolved directly by using the corresponding HMW combination (Hatch [27] 1982, Melbourne [28] 1985, and Wubbena [29] 1985). Because the geometric parameters and the ionosphere errors have been eliminated in this combination [30]. Then the integer ambiguity is resolved by rounding its float estimation to its nearest integer. Then the resolved integer ambiguity of EWL is put back into EWL to update the combination. The combination with resolved ambiguity can be regarded as more accurate pseudorange and be utilized in subsequent steps to resolve other combined ambiguities. With this information, the wide-lane (WL) combination is resolved by using the ambiguity-resolved EWL combination. The WL is combined by the second two closest L-band carriers and is supposed to have the second longest virtual wavelength. In relative positioning, the ionosphere errors are considered to have been eliminated by double difference between the satellites and receivers. Hence, the float estimation of the ambiguity is accurate enough to be rounded directly to get the integer ambiguity. With the first two ambiguity-resolved signals, the ambiguity of the third combination referred to as NL can be rounded in the way which is the same as the second step. The original observation with the longest wavelength is usually used as the NL combination directly in the traditional boot-strapping method. If each of the three combined virtual ambiguities is fixed correctly, the original ambiguities can then be reconstructed from the three first-order equations which are linearly independent to each other. Then they can be inserted back into the original positioning equations as known quantities to update the navigation results of the coordinates. Compared to other integer searching methods, the boot-strapping methods are regarded to have decreased the complexity of the computational steps a lot [22]. Without loss of generality, the boot-strapping method was first put forward for systems with triple-frequency carrier phases. However the principles are not restricted to

this situation and can be applied to other multi-frequency conditions.

IV. PROCEDURES OF THE IMPROVED METHOD

As illustrated in the previous section, no matter in which way the ambiguities are fixed to correct integers, first of all the float estimations are calculated such as they are resolved in the method of LAMBDA, TCAR, CIR and so on. Hence, the precision of the float ambiguity is the foundation for the following fixation procedures for most of the methods. With the estimation of the ambiguity being more precise, positioning accuracy in PPP will increase accordingly. So it is vital to improve the ambiguity resolution in PPP. Then the parameters of interest (e.g. coordinates of the receiver) can be calculated with higher precision. However, without being double-differenced first, the residual errors in PPP can't be eliminated directly as they are in the relative positioning. To increase the accuracy of the float ambiguities derived by boot-strapping method and remove the ionosphere delays which are simply omitted before, an improved method of integer ambiguity resolution for PPP is proposed in this section. This method is based on the traditional boot-strapping methods but is more adaptable for precise point positioning. By linear combinations, the virtual signals with longer wavelengths and lower noises can be constructed. Considering the characteristics of different combinations, the best virtual signals are chosen for AR according to their characteristics. In the previous boot-strapping methods, ionospheric errors are simply ignored due to the operation of double difference in relative positioning. However the ionospheric delays in PPP or in an active environment will be much larger. In other words, the combinations are biased by the residual ionospheric delays in addition to measurement and multipath noises. For decimeter or even centimeter precision positioning, the influence of the ionospheric delay with the magnitude of meter-scale is no doubt beyond endurance. If not eliminated, it will severely damage the estimation of the ambiguity. Hence, to reduce the ionospheric errors, extra pseudoranges are combined with the relatively better combinations in the improved method. Then through numerical test and analysis utilizing real GPS navigation data, the validity of the improved method for PPP is demonstrated. The ambiguity fixing results and the positioning precision of the improved method are compared with the traditional method. First of all, the modelling strategy for the PPP ambiguity resolution is considered. The boot-strapping methods designed for network positioning are modified so that they can be applied to the single point positioning.

For different GNSS systems, the wavelength, ionospheric scale factor, and the noise amplitude factor of the combination are different for each frequency-scheme. With variances of the combination coefficients k_1, k_2, and k_3, infinite combinations of the original observations can be constructed. However, due to bad characters such as amplification of ionospheric delays and noises along with even shorter wavelengths, most of the combinations are insufficient for precise point positioning. Hence, the selection of the combinations has a strong impact on the ambiguity resolution and positioning in PPP. In order to make a clear comparison of the characters among various combinations, the characteristics of the relatively valuable combinations of triple-frequency GPS are calculated and listed in Table 1 for reference. According to values of the three frequencies of GPS, the carriers are arranged as $L_1 = 1,575.420$ MHz, $L_2 = 1,227.600$ MHz and $L_3 = 1,176.450$ MHz as illustrated before. The characteristics of triple-frequency signals in other systems can be summarized in the same way. Hence, we can clearly compare the properties of different combinations and choose the optimal set of the combinations for ambiguity resolution and positioning.

A. PROCEDURES OF AMBIGUITY RESOLUTION

1) EWL COMBINATION

Usually, the two observations of the carrier phases whose frequencies are closer to each other than the other groups are selected in the first step. For GPS, the frequencies of carriers L_2 and L_3 are closer to each other. What's more, the wavelength of the combination $\Phi_{(0,1,-1)}$ is relatively larger, with ISF and PNF becoming lower as shown in Table 1. Hence, the combination coefficients of carriers L_2 and L_3 are assigned to be 1 and -1 in order to obtain longer wavelength. The combined ambiguity of this combination which is referred to as the EWL is supposed to be resolved first. The pseudorange observations on these two frequencies are combined by the coefficients of 1 and 1 referred to as the narrow-lane combination of the codes. The geometric parameters including the coordinates, receiver clock errors and the dry component of the tropospheric delays don't change with the frequencies. Hence they can be removed by subtraction between the narrow-lane combination of codes and the EWL combination of carrier phases which is integrally referred to as the HMW combination. Hence, the combined ambiguity and the combined ionospheric residuals are the left parameters to be resolved. The ambiguity of Φ_{EWL} derived by the HMW combination is indicated as:

$$\begin{aligned} N_{EWL} &= N_2 - N_3 \\ &= \frac{\frac{f_2P_2+f_3P_3}{f_2+f_3} - \frac{f_2\Phi_2-f_3\Phi_3}{f_2-f_3} - (\beta_{(0,1,1)} + \beta_{(0,1,-1)})\delta I_1}{\lambda_{EWL}} \end{aligned} \tag{15}$$

With $\beta_{(0,1,1)} = 1.7186$ and $\beta_{(0,1,-1)} = -1.7186$ as seen in Table 1, we can get that $\beta_{(0,1,1)} + \beta_{(0,1,-1)} = 0$. This result indicates that the combined ionospheric delay can be removed by the HMW combination directly. Furthermore, the combined wavelength has been amplified to 5.8610 m which is benefit to the resolution of the ambiguity. However, the PNF of this combination is becoming larger as 33.2415 according to Table 1 after combination. Suppose that the noise of the original carrier phase is 0.002 m as illustrated before, the value of the combined noise is still smaller than 0.1 m and obviously it is eligible to be ignored compared to the longer wavelength. The model errors such as the wet

TABLE 1. Characteristics of the triple-frequency combinations.

Combination	Characters			
$\Phi_{(k_1,k_2,k_3)}$	$f_{(k_1,k_2,k_3)}(GHz)$	$\lambda_{(k_1,k_2,k_3)}(m)$	$\beta_{(k_1,k_2,k_3)}$	$\mu_{(k_1,k_2,k_3)}$
$\Phi_{(1,0,0)}$	1.5754	0.1903	1	1
$\Phi_{(0,1,0)}$	1.2276	0.2442	1.6469	1
$\Phi_{(0,0,1)}$	1.1765	0.255	1.7933	1
$\Phi_{(0,1,-1)}$	0.0512	5.8610	-1.7186	33.2415
$\Phi_{(0,2,-1)}$	1.2788	0.2344	1.5123	2.1290
$\Phi_{(0,-1,2)}$	1.1253	0.2664	1.9529	2.3584
$\Phi_{(1,-1,0)}$	0.3478	0.8619	-1.2833	5.7400
$\Phi_{(2,-1,0)}$	1.9232	0.1559	0.5871	1.7583
$\Phi_{(4,-5,0)}$	0.1637	1.8316	-23.2604	53.7448
$\Phi_{(1,0,-1)}$	0.3990	0.7514	-1.3391	4.9282
$\Phi_{(2,0,-1)}$	1.9744	0.1518	0.5273	1.7035
$\Phi_{(77,-60,0)}$	47.6513	0.0063	0	2.9783
$\Phi_{(0,1,1)}$	2.4041	0.1247	1.7186	0.7073

component of the troposphere delays, satellite clock errors and so on are eliminated by precise models previously as expressed in the preceding part. Then the integer fixation of the EWL ambiguity is rounded from the float estimation and expressed as:

$$\breve{N}_{EWL} = round[N_{EWL}] \tag{16}$$

2) WL COMBINATION

Through comparison among the rest combinations except EWL, the combination with relatively longer wavelength and lower ISF or PNF is utilized in this step and is named as the wide-lane (WL) combination. If we assume that the values of δI_1 and ε keep constant, the combined error will be smaller with relatively smaller amplification factor and is beneficial to higher accuracy of ambiguity resolution. Moreover, as we can see in equation (9), usually the ISF and PNF are smaller when the combination coefficients are smaller. Hence, when the properties of different combinations are close to each other, the smaller coefficients are preferable for AR. As a result, the combination $\Phi_{(1,-1,0)}$ with the smallest coefficient group is chosen as the WL due to its relatively better property as shown in Table 1. Then the combined EWL ambiguity calculated in the previous step is substituted back into the EWL combination to obtain precise and exact carrier phase observation with higher accuracy. To eliminate the geometric and ionospheric parameters in the WL combination, extra pseudoranges are included to resolve the ambiguity of the second combination besides the carrier phase observation with fixed ambiguity. Here the pseudorange (code) observation on carrier L_1 is utilized. The corresponding coefficients of the code observation and EWL combination are assumed to be a_1 and a_2. Then the ambiguity of the WL combination is derived as (17), as shown at the bottom of the next page:

In order to resolve the WL ambiguity, the geometry and ionospheric parameters which are also unknown need to be removed first. Due to this requirement, the relationship of a_1 and a_2 can be expressed as:

$$a_1 + a_2 - 1 = 0 \tag{18}$$

$$a_1 + a_2\beta_{EWL} - \beta_{WL} = 0 \tag{19}$$

According to Table 1, we can get that $\beta_{EWL} = \beta_{(0,1,-1)} = -1.7186$ and $\beta_{WL} = \beta_{(1,-1,0)} = -1.2833$ for GPS. Therefore the values of the coefficients are derived as $a_1 = 0.160$ and $a_2 = 0.840$. Then the WL ambiguity can be resolved by (17) and the fixation can be rounded from the float estimation.

3) MODIFIED NARROW-LANE COMBINATION

In traditional boot-strapping methods, usually $\Phi_{(0,0,1)}$ of GPS is chosen as the narrow-lane combination. However, the ionospheric residuals and noises of the traditional NL combination are larger than the first two combinations in PPP. The errors will violate the precision of the ambiguity resolution. In order to improve the performance of ambiguity resolution in PPP, a modified combination is chosen. On one hand, the modified narrow-lane combination named as MNL should be independent to the first two combinations. On the other hand, the coefficients of this combination should be as small as possible however still possessing relatively longer wavelength and lower noise. According to Table 1, $\Phi_{(4,-5,0)}$ is chosen as the MNL combination. In consideration of other combinations, even if they may have lower amplification factors of the noises, the fairly short wavelength is a disadvantage to the estimation of the ambiguity. What's more, the noises with even quite small values will be evident in this process and consequently are not negligible. Then the WL with fixed ambiguity and the modified MNL combination are combined to resolve the combined ambiguity.

Previously, the WL individually is combined with the NL and the combination is capable to remove the geometric parameters because it is assumed that the ionosphere delays after double difference are small enough to be omitted. However in PPP the ionosphere residuals which are not eliminated in advance will be absorbed by the ambiguity and influence the ambiguity estimation and positioning. With observation data provided by IGS, the approximate values of the ionospheric errors can be derived out. The observation data of 400 epochs with a sampling interval of 30s is utilized. It is collected on January 1st 2017. Figure 1 depicts the ranges of the ionospheric delays of the signals on frequency f_1 of two GPS satellites. The PRN of the satellites are 26 (blue) and 27 (red) respectively. The PRN represents the unique number of a satellite [31]. Figure 1 shows that for the epochs before 150, the ionospheric errors of PRN 27 decrease from 3 m to 1.8 m and the errors of PRN 26 decrease from 2.5 m to 1.5 m. During the epochs of 200 to 400, the errors of both of the two satellites increase from about 1.6 m to 2.6 m approximately. As it is known, the ionospheric errors are related to the zenith-delay and the variance of the elevation

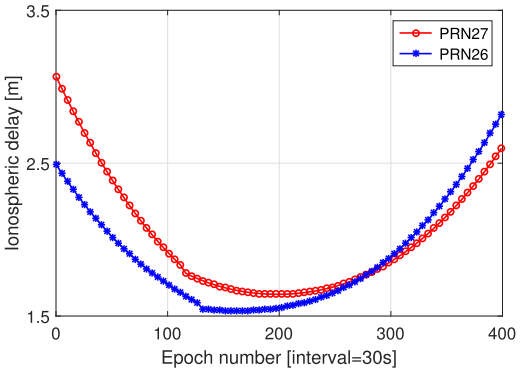

FIGURE 1. The ionospheric delays of the carrier phase L_1. The curves of blue and red correspond to the results of GPS satellites PRN 26 and PRN 27 respectively.

angle of the satellite. For a static receiver, the zenith-delay of the ionospheric error is relatively stable during a short time. Hence the errors will be smaller when the elevation angle of the satellite is larger. With the movement of the satellite, the elevation angle of the satellite will change accordingly and lead to the variance of the ionospheric delays for some extent. In summary, the values of the ionospheric errors usually are around meter-level as shown in Figure 1. Obviously the ionosphere delays can't be simply omitted for precise point positioning if they haven't been removed in advance. Therefore, in order to remove the geometric and ionospheric parameters, N_{MNL} is derived by including the pseudorange observations along with the fixed WL combination and is expressed as (20), as shown at the bottom of the next page:

The combination coefficients are subjected to the conditions as:

$$b_1 + b_2 - 1 = 0 \tag{21}$$

$$b_1 + b_2\beta_{WL} - \beta_{MNL} = 0 \tag{22}$$

According to Table 1, we can get that $\beta_{WL} = \beta_{(1,-1,0)} = -1.2833$ and $\beta_{MNL} = \beta_{(4,-5,0)} = -23.2604$ for GPS. Therefore the values of the coefficients are derived as $b_1 = -9.625$ and $b_2 = 10.625$. Although the ISF of MNL combination is larger than that of the NL as seen in Table 1, the wavelength has also increased a lot. What's more the ionospheric delays are eliminated by combining the pseudorange and carrier phase observations with the coefficients of b_1 and b_2. Hence the ISF won't be included in the resolution equation. And the combination leads to a quite small b_1 which is also beneficial for AR because the pseudorange measurement relatively has larger noises than the carrier phase observation. At last the fixation of MNL ambiguity is rounded from the float estimation directly.

B. RESOLUTION OF ORIGINAL AMBIGUITIES

Once the three combined ambiguities have been resolved, the original ambiguities of the triple-frequency carrier phases can be recovered from the linear equations composed by the combined ambiguities. According to the coefficients of the EWL, WL and MNL when combining the original ambiguities, the equations are expressed as:

$$\begin{bmatrix} 0 & 1 & -1 \\ 1 & -1 & 0 \\ 4 & -5 & 0 \end{bmatrix} \begin{bmatrix} N_1 \\ N_2 \\ N_3 \end{bmatrix} = \begin{bmatrix} N_{(EWL)} \\ N_{(WL)} \\ N_{(MNL)} \end{bmatrix} \tag{23}$$

As we can see, the equations are independent to each other. Hence, unique solutions can be resolved from the equations of full rank. After the ambiguities have been fixed, the exact values of the carrier phases can be calculated by combing the ambiguity integers with the fractional parts generated by the receiver previously. The fixed carrier phases are regarded as range parameters and are put back into the positioning equations to achieve more precise positioning results of PPP.

V. NUMERICAL TEST AND ANALYSIS OF REAL DATA

Nowadays real triple-frequency data of GNSS provided by the IGS is available online and accessible to users. The triple-frequency observations utilized in this test are collected on January 1st, 2017 by the DUMN station of IGS. The observation interval of this static receiver is 30s. First, with observations of satellite PRN 26 and PRN 27, we calculate the success rates of the combinations to verify the validity of the method in a theoretical aspect. Then the residuals of the combined ambiguities contrast to the reference ones are resolved and depicted in figures. The results of NL in the traditional method is also listed to show a comparison of the two methods. At last, the combined ambiguities of both the two methods are substituted back into the observation equations to resolve the coordinates of the station. The results compared to the standard coordinates given in the positioning file of IGS are pictured. In this test, the accurate coordinates of the stations have already been calculated by IGS and are provided in the files of IGS for reference.

A. SUCCESS RATES OF VARIOUS COMBINATIONS

According to the process of estimating the combined ambiguities, it is shown that they will be biased by the combined ionospheric delay $\beta_{(k_1,k_2,k_3)}\delta I_1$ before the errors have been removed thoroughly, along with the variance of $\sigma_{N_{(k_1,k_2,k_3)}}$. In common situation, the noises are assumed to be normally distributed. Hence, the ambiguity of the extra-wide-lane combination meets the distribution of $N_{EWL} \sim N(\beta_{EWL}\delta I_1, \sigma_{N_{EWL}})$. Similarly, the ambiguity estimations of the WL, MNL and NL combinations obey the identical distribution with the biases and variances corresponding to their

$$N_{WL} = \frac{(a_1P_1 + a_2\Phi_{EWL} - \Phi_{WL}) + (a_1 + a_2\beta_{EWL} - \beta_{WL})\delta I_1 + \lambda_{EWL}N_{EWL}}{\lambda_{WL}} \tag{17}$$

own combined ionospheric delays and noises respectively. Although the real situation may be slightly different from these conditions, the assumptions are valid in most cases as illustrated in the previous work. With the noise and residual ionospheric delay being the variance and bias respectively, the probability between the boundaries of -0.5 cycle and 0.5 cycle can be regarded as the theoretical success rate of the ambiguity resolution. Because the residual with an absolute value larger than 0.5 cycle will more likely lead to an incorrect result. In conclusion, the success rate of the combined ambiguities can be derived by the Gaussian probability density function and is written as:

$$P(-0.5 < x < 0.5) = \int_{-0.5}^{0.5} \frac{1}{\sqrt{2\pi}} exp\left(-\frac{(x-\mu)^2}{2\sigma^2}\right) dx \tag{24}$$

where x represents the difference between the float ambiguity estimation and the reference value calculated from the precise data given by the file of IGS previously. μ and σ indicate the bias and variance of x in cycles respectively. Obviously even for the same combinations, the success rate will be influenced by the magnitude of the residual ionospheric delays and the noises of the observations. Hence, the success rates of the combinations can be utilized to demonstrate the performance of the improved method.

Through changing the values of the ionospheric delays and noises, we can depict the variances of the success rates of different ambiguity combinations. As illustrated before, the measurement noises on different frequencies are identical to each other. Under common situations, the standard deviations of the pseudorange and carrier phase observations are usually meter-scale and centimeter-scale to millimeter-scale, respectively [26]. The ionosphere errors and the standard deviations are calculated by equations (9) and (13).

Figure 2 (a), (b), (c) and (d) plot the success rates of the EWL, WL and MNL ambiguities of the improved method along with the NL ambiguity of the traditional method. The results of different colors in each of the pictures represent the condition of different standard variances. The red curve represents the condition of $\sigma_\Phi = 0.002$ m. The dark blue and light blue curves correspond to the variances of $\sigma_\Phi = 0.008$ m and $\sigma_\Phi = 0.02$ m respectively. The wide range of the three different values is capable to represent most of the conditions that the positioning process will meet. The horizontal and vertical axes of Figure 2 represent the ranges of ionosphere delays of carrier L_1 and the success rates of the combined ambiguities respectively. For each subgraph, the success rates of the ambiguity estimations gradually decrease with the increment of ionospheric delays. The curves with larger standard variances drop faster than the ones with smaller noises for the same combination. As Figure 2 (c) shows, the success

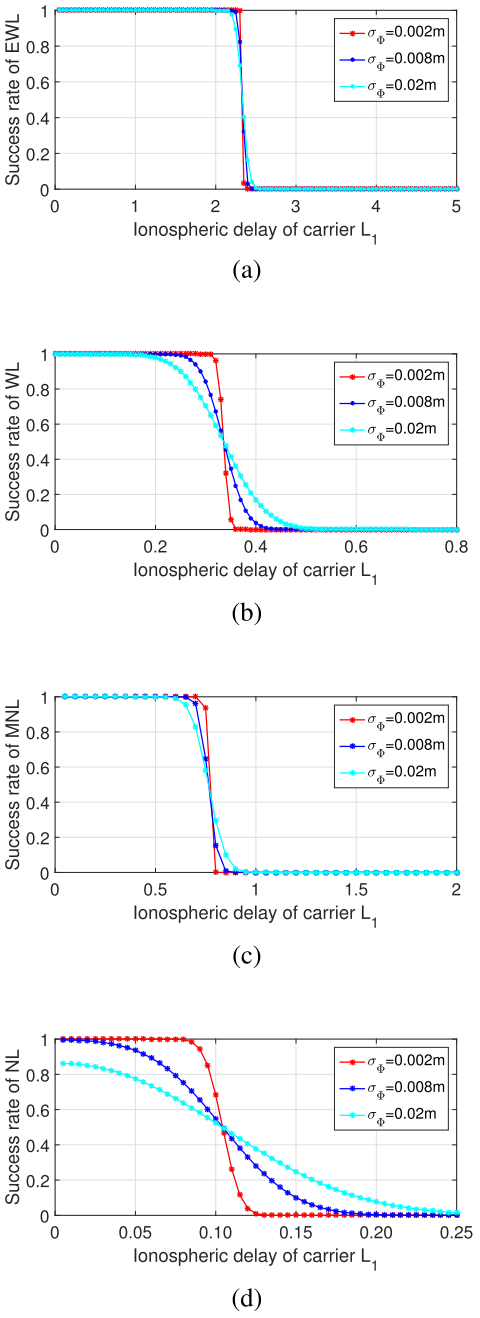

FIGURE 2. The success rates of EWL, WL, MNL and NL versus the ionospheric delays of carrier L_1 with different noises.

rate of the MNL ambiguities won't drop below 99.9% until the ionospheric delay is larger than 0.6 m even under the quite noisy situation with $\sigma_\Phi = 0.02$ m. However even under very quiet environment with the smallest noise of $\sigma_\Phi = 0.008$ m, the success rate of the NL ambiguities of the traditional method quickly drops to zero when the ionosphere delay is

$$N_{MNL} = \frac{(b_1 P_1 + b_2 \Phi_{WL} - \Phi_{MNL}) + (b_1 + b_2 \beta_{WL} - \beta_{MNL})\delta I_1 + \lambda_{WL} \triangle N_{WL}}{\lambda_{MNL}} \tag{20}$$

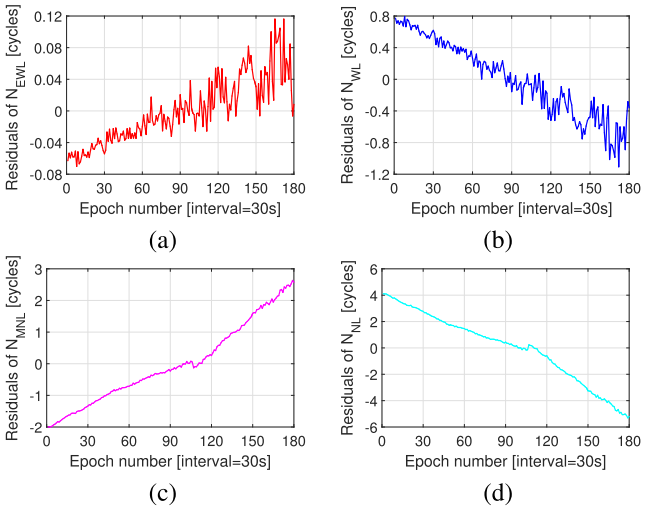

FIGURE 3. The ambiguity residuals of EWL, WL, MNL and NL combinations of PRN 26 in cycles.

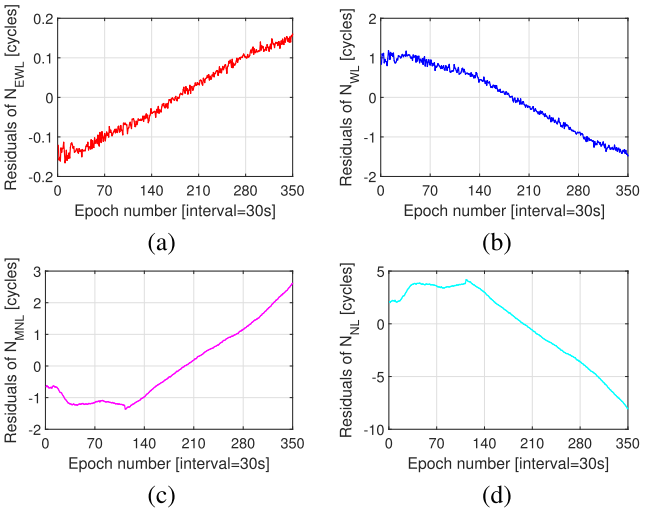

FIGURE 4. The ambiguity residuals of EWL, WL, MNL and NL combinations of PRN 27 in cycles.

as small as 0.12 m. As it is shown in Figure 1, the magnitude level of the ionospheric errors surely will exceed this threshold. Therefore, the ranges of the success rates indicate that, compared to the improved method, the traditional method is more inclined to be influenced by the ionosphere delays and the noises which are the main obstacles in PPP. In a similar way we can plot the success rates of other combinations, and the results validate that the EWL and WL combinations do possess the best and second best properties when compared to other frequency-schemes. What's more, consistent to the theoretical derivation in the preceding part, the MNL combination does have relatively better properties than the other remaining combinations.

B. RESIDUALS OF AMBIGUITY ESTIMATIONS

After verifying the theoretical success rate, we employ real observation data into the procedures of the improved and traditional methods to calculate the values of the combined ambiguities. With the precise coordinates of the station given by the positioning files of IGS, the value of the referenced ambiguities can be derived in advance. The differentials between the computed ambiguities and the referenced ones are defined as the ambiguity residuals which indicate the performance of the AR method. Smaller residual means higher precision of ambiguity estimation. In this test, the observation data of satellites PRN 26 and PRN 27 are utilized. Figure 3 (a), (b) (c) and (d) depict residuals of the EWL, WL, MNL and NL combined ambiguities of PRN 26. During the observation time of 180 epochs with the sampling interval of 30s, the absolute values of the N_{EWL} and N_{WL} residuals don't exceed 0.15 cycle and 1.3 cycles respectively which indicate accurate estimations of the two combined ambiguities. Although the residuals of N_{MNL} are larger than the previous two combinations, they have achieved better results than the NL ones of the traditional method as shown in Figure 3 (c) and (d). Figure 4 (a), (b), (c) and (d) illustrate the combined ambiguity residuals of satellite PRN 27. The curves of the subgraphs show the similar tendencies and results as the ones of PRN 26. Residuals of other satellites can be calculated in the same way and the results showing the same tendency are not depicted for clearness. Hence, the ambiguity resolution of the improved method is supposed to possess better precision than the traditional one.

C. RESIDUALS OF POSITIONING RESULTS

As illustrated in the preceding section, the original ambiguities are recovered by linearly independent equations composed by the combined ambiguities which have been resolved. Then, the ambiguity estimations are put back into equation (2) to achieve more accurate coordinates of the receiver. Because the range parameters which are calculated by the C/A codes previously and utilized to resolve the coordinates are replaced by more accurate carrier phases, the positioning results are supposed to have higher accuracy. The reference positioning coordinates of the stations are provided by the navigation files of IGS in advance. Then the positioning results of the two methods are calculated through using the carrier phases with fixed ambiguities. Both the results are compared with the accurate location information given in advance to inspect the positioning precision respectively. The coordinates of the stations contain three components which are in the east, north and up directions (ENU). Figure 5 (a), (b) and (c) illustrate the positioning residuals of the three components. Both the results of the improved method (red) and the traditional method (blue) are depicted. As it is shown, the positioning errors of the improved method have decreased for most of the epochs when compared to the traditional method in each of the three directions. The improvement in the up direction isn't as obvious as it is in the other two directions. It can be interpreted that maybe the ambiguities of the carrier phases are not the main factors that influence the coordination of this direction. What's

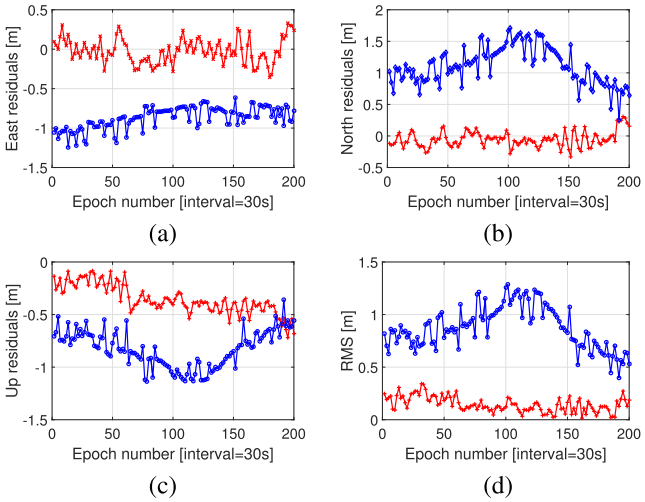

FIGURE 5. The positioning residuals in the east, north and up directions (a, b and c) and the integral RMS of the traditional (blue) and improved (red) methods.

TABLE 2. Mean values and RMS of the ambiguity and positioning residuals.

	N residuals		Coordinate residuals			
	PRN 26	PRN 27	x [m]	y [m]	z [m]	RMS [m]
Traditional	-0.36	1.75	0.26	0.33	-0.51	0.32
Improved	0.61	4.23	-0.73	0.82	-0.71	0.81
Increase	41.0%	58.6%	64.4%	59.8%	28.2%	60.5%

more, the results close to the epoch 200 are relatively bad. This condition maybe is caused by the transforming of the satellite constellation and the initialization will be affected as a result. However, the integral tendency of decrease of the positioning residuals indicates that the ambiguity estimations of the improved method are more precise than that of the traditional one. It indicates that the improved AR method has more efficient performance and can achieve higher success rate under the same environment conditions. Figure 5 (d) depicts the RMS of the integral residuals of the two methods. In conclusion, the numerical characters of the results are listed in Table 2. The results of the traditional and improved methods are listed in the first and second rows respectively. The N residuals of PRN 26 and PRN 27 in the second and third columns represent the mean values of the MNL and NL combinations respectively. RMS of the solution in the three directions along with the integral values are listed in the columns 4-7. The third row of Table 2 shows the value of increment.

VI. CONCLUSION

Precise point positioning is widely utilized in many fields. The accurate estimation of the integer ambiguity of the carrier phase is regarded as a precondition of precise positioning. With triple-frequency signals of GNSS being accessible, we put forward an improved method in order to achieve more precise estimations of the ambiguities and positioning results in PPP. Combinations of the original observations are constructed to obtain better characters which are beneficial for ambiguity resolution, such as longer wavelengths and lower measurement noises. Through sufficient comparison of the combined characters, the EWL, WL and MNL combinations with relatively better properties are chosen for AR. In PPP, the ionospheric error is not small enough to be omitted as it is in traditional boot-strapping method. Therefore, to resolve the combined ambiguities, extra pseudorange measurements are employed in the combination to make it capable to reduce the ionospheric delays along with the geometric parameters. Real triple-frequency observations of GPS provided by IGS are utilized in the numerical test. To demonstrate the efficiency of the improved method, the ambiguity and positioning residuals along with the success rates of the two methods are calculated with reference to the precise values given by the navigation file in advance. The test results show that the ambiguity combinations of the improved method have higher success rates. What's more, residuals of the ambiguity and the coordinate estimations have decreased. In summary, the consequences indicate that the improved method is efficient to increase the accuracy of the ambiguity resolution and the positioning results.

REFERENCES

[1] X. Gong, Y. Lou, W. Liu, F. Zheng, S. Gu, and H. Wang, "Rapid ambiguity resolution over medium-to-long baselines based on GPS/BDS multi-frequency observables," *Adv. Space Res.*, vol. 59, no. 3, pp. 794–803, 2017.

[2] J. Kouba and P. Héroux, "Precise point positioning using IGS orbit and clock products," *GPS Solutions*, vol. 5, no. 2, pp. 12–28, 2001.

[3] S. Bisnath and Y. Gao, "Current state of precise point positioning and future prospects and limitations," in *Observing our Changing Earth*. Berlin, Germany: Springer, 2009, pp. 615–623.

[4] J. F. Zumberge, M. B. Heftin, D. C. Jefferson, M. M. Watkins, and F. H. Webb, "Precise point positioning for the efficient and robust analysis of GPS data from large networks," *J. Geophys. Res., Solid Earth*, vol. 102, no. B3, pp. 5005–5017, 1997.

[5] M. Soycan and E. Ata, "Precise point positioning versus traditional solution for GNSS networks," *Sci. Res. Essays*, vol. 6, no. 4, pp. 799–808, 2011.

[6] G. Blewitt, "Carrier phase ambiguity resolution for the global positioning system applied to geodetic baselines up to 2000 km," *J. Geophys. Res., Solid Earth*, vol. 94, no. B8, pp. 10187–10203, 1989.

[7] J. Geng, F. N. Teferle, C. Shi, X. Meng, A. H. Dodson, and J. Liu, "Ambiguity resolution in precise point positioning with hourly data," *GPS Solutions*, vol. 13, no. 4, pp. 263–270, 2009.

[8] J. Geng, "Rapid integer ambiguity resolution in GPS precise point positioning," Ph.D. dissertation, Dept. Civil Eng., Univ. Nottingham, Nottingham, U.K., 2011.

[9] S. Banville, P. Collins, and F. Lahaye, "GLONASS ambiguity resolution of mixed receiver types without external calibration," *GPS Solutions*, vol. 17, no. 3, pp. 275–282, 2013.

[10] J. Geng *et al.*, "Improving the estimation of fractional-cycle biases for ambiguity resolution in precise point positioning," *J. Geodesy*, vol. 86, no. 8, pp. 579–589, 2012.

[11] J. Geng, X. Meng, A. H. Dodson, and F. N. Teferle, "Integer ambiguity resolution in precise point positioning: Method comparison," *J. Geodesy*, vol. 84, no. 9, pp. 569–581, 2010.

[12] X. Li, M. Ge, H. Zhang, and J. Wickert, "A method for improving uncalibrated phase delay estimation and ambiguity-fixing in real-time precise point positioning," *J. Geodesy*, vol. 87, no. 5, pp. 405–416, 2013.

[13] M. Ge, G. Gendt, M. Rothacher, C. Shi, and J. Liu, "Resolution of GPS carrier-phase ambiguities in precise point positioning (PPP) with daily observations," *J. Geodesy*, vol. 82, no. 7, pp. 389–399, 2008.
[14] X. Zhang, P. Li, and F. Guo, "Ambiguity resolution in precise point positioning with hourly data for global single receiver," *Adv. Space Res.*, vol. 51, no. 1, pp. 153–161, 2013.
[15] B. Zhang, P. J. G. Teunissen, and D. Odijk, "A novel un-differenced PPP-RTK concept," *J. Navigat.*, vol. 64, no. S1, pp. S180–S191, 2011.
[16] W. Bertiger *et al.*, "Single receiver phase ambiguity resolution with GPS data," *J. Geodesy*, vol. 84, no. 5, pp. 327–337, 2010.
[17] A. Q. Le, C. C. J. M. Tiberius, H. van der Marel, and N. Jakowski, "Use of global and regional ionosphere maps for single-frequency precise point positioning," in *Observing Our Changing Earth*. Berlin, Germany: Springer, 2009, pp. 759–769.
[18] P. J. G. Teunissen, D. Odijk, and B. Zhang, "PPP-RTK: Results of cors network-based PPP with integer ambiguity resolution," *J. Aeronaut., Astronaut. Aviation, A*, vol. 42, no. 4, pp. 223–230, 2010.
[19] E. Kaplan and C. Hegarty, *Understanding GPS: Principles and Applications*. Norwood, MA, USA: Artech house, 2005.
[20] Y. Gao and K. Chen, "Performance analysis of precise point positioning using rea-time orbit and clock products," *J. Global Positioning Syst.*, vol. 3, nos. 1–2, pp. 95–100, 2004.
[21] A. Xu, Z. Xu, M. Ge, X. Xu, H. Zhu, and X. Sui, "Estimating zenith tropospheric delays from beidou navigation satellite system observations," *Sensors*, vol. 13, no. 4, pp. 4514–4526, 2013.
[22] P. Teunissen, P. Joosten, and C. Tiberius, "A comparison of TCAR, CIR and LAMBDA GNSS ambiguity resolution," in *Proc. 15th Int. Tech. Meeting Satellite Division Inst. Navigat. (ION GPS)*, 2003, pp. 2799–2808.
[23] B. Forssell, R. Harris, and M. Martin-Neira, "Carrier phase ambiguity resolution in GNSS-2," in *Proc. ION GPS*, vol. 10. 1997, pp. 1727–1736.
[24] R. Hatch, J. Jung, P. Enge, and B. Pervan, "Civilian GPS: The benefits of three frequencies," *GPS Solutions*, vol. 3, no. 4, pp. 1–9, 2000.
[25] M. Soycan, "A quality evaluation of precise point positioning within the bernese GPS software version 5.0," *Arabian J. Sci. Eng.*, vol. 37, no. 1, pp. 147–162, 2012.
[26] A. R. Amiri-Simkooei, S. Jazaeri, F. Zangeneh-Nejad, and J. Asgari, "Role of stochastic model on GPS integer ambiguity resolution success rate," *GPS Solutions*, vol. 20, no. 1, pp. 51–61, 2016.
[27] R. Hatch, "The synergism of GPS code and carrier measurements," in *Proc. Int. Geodetic Symp. Satellite Doppler Positioning*, vol. 1, 1983, pp. 1213–1231.
[28] W. G. Melbourne, "The case for ranging in GPS-based geodetic systems," in *Proc. 1st Int. Symp. Precise Positioning Global Positioning Syst.*, vol. 1519, 1985, pp. 373–386.
[29] G. Wübbena, "Software developments for geodetic positioning with gps using ti-4100 code and carrier measurements," in *Proc. 1st Int. Symp. Precise Positioning Global Positioning Syst.*, 1985, pp. 403–412.
[30] W. Tang, C. Deng, C. Shi, and J. Liu, "Triple-frequency carrier ambiguity resolution for Beidou navigation satellite system," *GPS Solutions*, vol. 18, no. 3, pp. 335–344, 2014.
[31] G. Xu and Y. Xu, *GPS: Theory, Algorithms and Applications*. Berlin, Germany: Springer, 2016.

XIAOYING GU received the bachelor's degree from Beijing Jiaotong University in 2013. She is currently pursuing the Ph.D. degree with the School of Electronics Engineering and Computer Science, Peking University, Beijing, China. Her current research interests include multifrequency and multisystem algorithms of ambiguity resolution and precise point positioning.

BOCHENG ZHU received the Ph.D. degree in electromagnetic field and microwave technology from the Beijing Institute of Technology, Beijing, China, in 1996. He is currently a Professor with the School of Electronics Engineering and Computer Science, Peking University, Beijing. He is a Senior Member of the Chinese Institute of Electronics. His research interests include wireless communication, satellite navigation, and microwave technology. He is a Senior Reviewer for the National High Technology Research and Development Program (863 Program) and the National Science and Technology Major Project of China.